Indian J. Phys. **67B** (6), 503 – 509 (1993)

Resonance Raman scattering

G Basavaraju
Physics Department, Indian Institute of Technology, Bombay, India

Abstract : Resonance scattering and Resonance Raman scattering in the context of inelastic scattering of photon by inner shell electron are distinguished. The status of theoretical calculations are outlined. The scenario in the experimental studies on Resonance Raman scattering and some recent results are presented The future theoretical and experimental investigations desired to be persued are highlighted.

Keywords : Photon scattering, resonance Raman scattering

PACS No. : 32 80 –t

1. Introduction

Inelastic photon scattering from inner shell electrons forms an integral part of the scattered photon spectrum. When scattering leads to ionisation of the participating atom, the scattering process is called Compton Scattering. Raman scattering involves the excitation of a struck electron to a higher energy unoccupied bound state. The same term has also been used occasionally in situations in which the struck electron is excited to vacant state within the conduction band in solids. In this review the focus will be on such situation in which the incident photon energy is slightly less than the binding energy of an inner shell electron. In such situation a large enhancement on the inelastic scattering is seen (Sparks [1]; Bennett and Freund [2]). A theoretical frame work for an understanding of these observations has been published sometime back by Gavrila and Tugulea [3]. Whether the final electron is in an excited bound state, or in a continuum, the term Resonance Raman Scattering (RRS) has been usually employed to designate the enhancement in both situations.

In available tabulation of photon attenuation coefficients, the contribution of resonant scattering has not been included even at energies close to absorption edges.

In the following sections, a theoretical understanding of the process, the results of experimental studies done so far and the future outlook are outlined.

2. Theoretical understanding

The concept underlying K-L RRS is illustrated in Figures 1a and 1b, the first referring to an isolated atom and the second to an atom in a solid. A K-shell electron is virtually excited to a continuum state of kinetic energy ε_e which is above the zero energy level in the case of an isolated atom and above the Fermi energy E_F in the case of a solid. An L-shell electron fills up the K-shell hole with the emission of a photon of energy $h\nu_f$. Since $h\nu_i$ is assumed to be less than the K-shell electron binding energy B_K, the K-shell hole state in RRS is off the energy shell. This means, in the perturbation methods of analysis of the process, second order matrix elements of $\boldsymbol{A}.\boldsymbol{P}$. interaction term are essential. The final state consists of a photon, a p-wave electron of kinetic energy ε_e and a hole in an outer shell. If the binding energy of the final state hole is represented as B_L or B_M, for simplicity, the requirement of energy conservation in RRS leads to

$$h\nu_i = h\nu_f + B_L \left(\text{or } B_M\right) + \varepsilon_e$$

for K–L (or K–M) RRS.

The calculation of cross section for RRS begins with the evaluation of matrix elements for $\boldsymbol{A}.\boldsymbol{P}$. term of interaction hamiltonian in the second order, which involves summation over intermediate states. When the incident energy is close to $E_n - E_i$, where i and n refer to the initial and intermediate states of the electron, resonance enhancement takes place. Considering only the dominant contribution and dipole approximation, it is possible to arrive at double differential cross section $\left[d^2\sigma/d\Omega\, dh\nu_f\right]_{\text{RRS}}$ for K–L RRS in terms of the photoelectric cross section evaluated at $\left(B_K + \varepsilon_e\right)$, where B_K is the K-shell binding energy and ε_e is the electron energy and certain radial integrals involving radial wave function for the relevant electrons (Cooper [4]).

Aberg and Tulkki in 1985 [5], have shown that a small anisotropy and polarization dependence of RRS to result from the interference between resonant and non-resonant terms in the complete matrix element. Theoretical investigation of anisotropy and polarization dependency of RRS at incident photon energy near L_3 is needed, since the intermediate L_3 vacancies are not spherically symmetric. The double differential cross section for K–L RRS shows a sharp rise as $h\nu_f$ decreases through $(h\nu_i - B_L - E_F)$ and sufficiently below this cut off decreases approximately as $h\nu_f\,(B_K - B_L - h\nu_f)^{-2}$. The calculated asymmetric line shape below cut off has been verified. Similar remarks will be applicable in the case of $K \rightarrow M$ or $K \rightarrow N$ with B_M and B_N in the place of B_K in the above expression. It should be noted that as the incident photon energy exceeds the K-shell threshold, RRS goes over into K X-ray fluorescence.

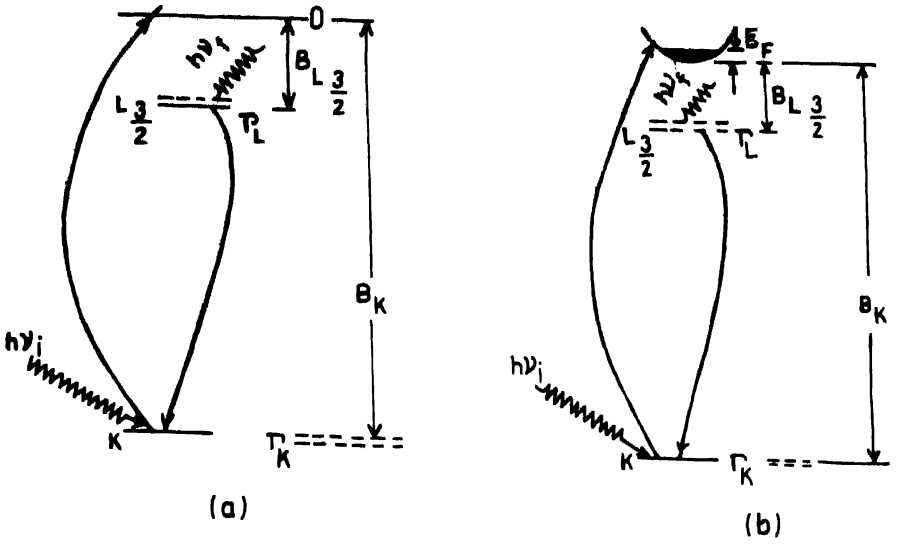

Figure 1. Schematic representation of K–L_3 resonant Raman scattering of X-rays of energy $h\nu_i$ near a K-shell threshold; (a) for an isolation atom an (b) for an atom in a solid. See also section 1 for a discussion of terminology. The energy of the scattered photon is indicated by $h\nu_f$. The widths of the virtual K-shell hole state and of the final L_3-subshell hole state are Γ_K and Γ_L respectively. The binding energies of the K-shell and the L_3-subshell are labelled as B_K and $B_{L3/2}$ respectively. E_F is the Fermi energy

3. Experiments and experimental data

Early experiments used X-rays generators with suitable monochromators. Synchrotron radiation sources (SRS) with various monochromatising techniques, which can produce narrow divergence (< 0.1 mrad) and small energy spread (< eV) have come into existence. These SRS are particularly suitable for RRS studies on account of tunability and strong linear polarization in the plane of electron orbit.

In studies of resonant scattering near for example K-shell thresholds, attention is mainly focused on scattered beam spectrum near $(h\nu_i - B_L)$ or $(h\nu_i - B_M)$, *i.e.*, near the photon energies comparable to appropriate photo electron energies. Since bremsstrahling intensity in the tip region is small, targets of fair thickness can be used. However, pure targets are essential in order to ensure the absence of characteristic X-rays of impurities of slightly lower Z. Modern detectors of high efficiency and good energy resolution have improved the quality of recent experiments manifold. Double crystal Bragg spectrometer with 0.8 eV resolution have been used by Eisenburger *et al* in 1976 [6].

The incident energy is varied in the neighbourhood of a target atom relevant binding energy. K X-ray yield for incident energy just above the threshold is used to determine the incident beam intensity. Thus, absolute values of resonant scattering cross sections can

be determined without having to measure directly the absolute value of incident beam intensity.

Various experiments have been presented in a tabular form in a recent article by Kane [7]. Salient features like source, target, geometrical details and brief comments regarding the nature of results are given different columns. This form is expected to assist the reader in assessment of the overall situation.

Illustrative resonant scattering spectra, obtained by Etalaniemi *et al* in 1988 [8], with a Si(Li) detector in the case of scattering of monochromatised synchrotron radiation of different energies through 90° by a copper target, are exhibited in Figure 2. Shapes of pulse height

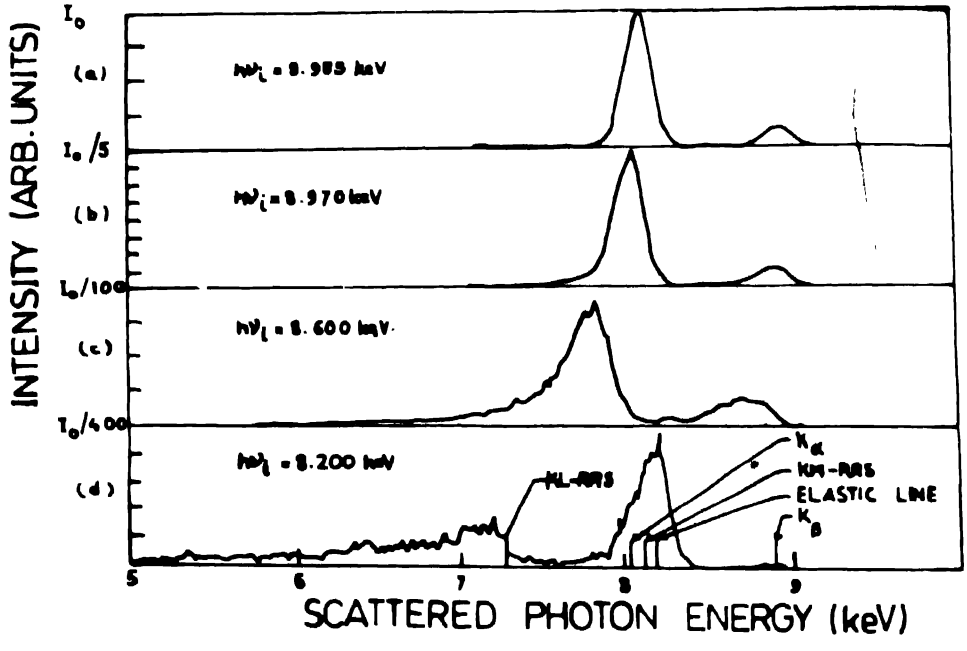

Figure 2. Resonant Raman scattering spectra obtained with a copper target and with different energies of monochromatised X-rays at the Daresbury synchrotron radiation source [8]. The *K*-shell threshold of copper is at 8 980 keV. Part (a) of the figure shows a large intensity of fluorescent K_α and K_β X-rays of copper. Note the scales of I_0, $I_0/5$, $I_0/100$ and $I_0/400$ for the parts (a), (b), (c) and (d) respectively. The shift in the RRS peak towards lower energies with decreasing $h\nu_i$ and a composite peak in part (d) near the elastic line should be noted. When $h\nu_i$ is lower than 8.980 keV, K_α and K_β X-ray contributions can still arise due to harmonics passed by the monochromator in the incident beam.

spectra of K_α and K_β X-ray can be seen in the topmost portion of the figure for 8.955 keV incident energy which is larger than the *K*-shell binding energy. Weak K_α and K_β indicated in the lowest portion of the figure are due to small intensities of harmonics passed by the monochromator.

4. Discussion of the results

From Figure 2 we see that as the incident energy is reduced, the scattered intensity decreases, and the downward shifted peaks show an asymmetry and also larger widths. The decrease of the intensity and the shapes are in accordance with the theoretical expectations on the basis of dipole approximation and the results thereof. On the scale of the lowest part of the figure the elastic line, the K–M RRS and the K_α X-rays caused by weak harmonics passed by the monochromator result in a composite unresolved peak.

A thorough analysis of the main features of RRS was presented some time ago by Eisenberger *et al* [6,9]. In the initial work with a semiconductor detector, the peak position shifted linearly with $h\nu_i$ when $(B_K - h\nu_i)$ was larger than about 40 eV but the apparent change in peak position was faster as $h\nu_i$ approached close to B_K from below. These observed variations in peak positions were shown to arise from the insufficient detector resolution and the changing shape of the RRS spectrum. In the subsequent high resolution experiments, the RRS peak position was seen to shift linearly with $h\nu_i$ as expected. Further, the energy integrated RRS intensity was, as expected, proportional to

$$\tan^{-1}\left[\Gamma_K/2\left(B_K - E_F - h\nu_i\right)\right].$$

Since the K-shell hole state is involved only virtually in RRS, the corresponding line width is determined by the incident beam energy spread and the final state width. Then RRS line width can be even smaller than the lifetime limited widths of the K-shell fluorescence as the latter involves real K-shell hole state width. A detailed theory of this line narrowing in RRS spectra has been presented by Aberg and Tulkki (1985).

From similar studies, Hamalainen *et al* [10] were able to determine widths of K-shell hole states in Cu, Zn and of L_3 hole state in Ho, Yb and Ta. Isotropic character of K–M RRS in Mo has been confirmed within experimental errors by Kodre and Shafroth [11], and so also the shape of K–M RRS in Yb by Manninen *et al* in 1985 [12].

Figure 3 shows the data obtained by Schaupp *et al* [13] for Nd target (B_K = 43.57 keV), after subtraction of Compton scattering contribution. For the first time K–N RRS was clearly seen. Further, K–L_2 and K–L_3 RRS contributions were resolved. Solid lines indicate the double differential cross section calculated in non relativistic, dipole approximation but with relativistic expressions for the K-shell photo effect cross section and the relevant electron wave functions. Polarization insensitiveness of K–L RRS in xenon has been established by choosing the plane of scattering parallel and perpendicular to the incident beam.

Quantitative agreement between experiment and theory in the case of both K–L and K–M RRS intensities implies that the K_α and K_β branching ratio known from K X-ray fluorescence is also applicable for the relative intensities of K–L and K–M RRS. Approximate constancy of radiative yield both below and above the threshold energy B_K has been demonstrated in studies with Ni by Manninen [14] and in Kr by Kodre *et al* [15]. These and

the results mentioned above provide an experimental confirmation of the assumptions underlying the simple theory outlined earlier.

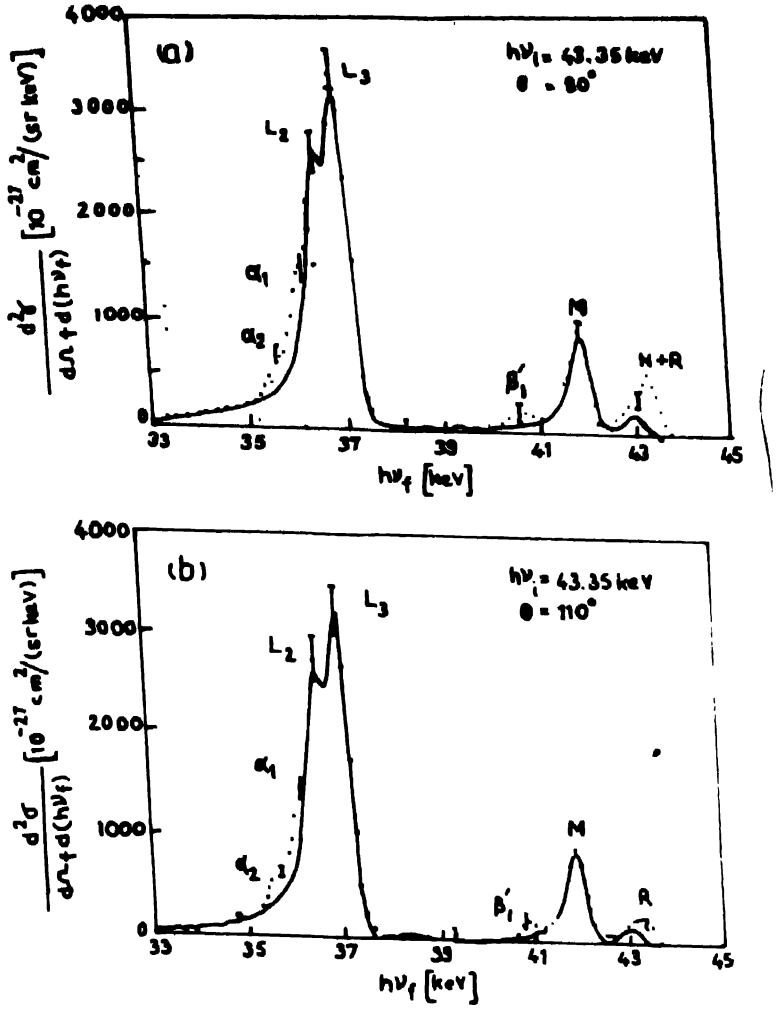

Figure 3. Double differential cross sections of neodymium atoms for resonant Raman scattering of 43.35 keV synchrotron radiation; (a) through 80° and (b) through 110°, obtained by Schaupp *et al* (1984) after subtraction of the usual Compton contribution. The binding energy B_K of the K-shell is 43.57 keV in this case. The symbol R indicates elastic scattering. Peaks marked α_1, α_2, β'_1 represent characteristic K X-rays of a minute praseodymium impurity. The solid curve shows the calculation of Schaupp *et al* [13] in the dipole approximation.

5. Conclusion and outlook

Intense, tunable, polarized and monochromatised radiation from synchrotron facilities have been recently used with advantage to investigate subtle features of resonance Raman

scattering of X-rays. The dipole approximation has been found to be successful in quantitative explanation of the main features of RRS cross section. It will be interesting to probe specific solid state environment effects in these phenomena with high resolution spectrometers. There is no information so far concerning the angular distribution of RRS of photons of energies close to L_3 subshell thresholds. Experiments involving coincidences between the resonantly scattered photons and the recoiling electrons should become possible with new synchrotron facilities being set up. Such experiments are expected to provide incisive probes on the range of validity of the dipole approximation.

Acknowledgment

The author gratefully acknowledges the helpful discussions with Prof. P P Kane and his permission to use some of his results.

References

[1] C J Spark 1974 *Phys. Rev* **A16** 221 *Lett* **33** 262

[2] Y B Bennett and I Freund 1975 *Phys. Rev Lett.* **34** 32

[3] M Gavrila and M N Tugulea 1976 *Rev. Roum. Phys.* **20** 209

[4] J W Cooper 1962 *Phys Rev.* **128** 681

[5] T Aberg and J Tulkki 1985 *Atomic Inner Shell Physics* ed B Crasemann (New York : Plenum) Ch 10

[6] P Eisenberger, P M Platzman and H Winick 1976 *Phys. Rev. Lett.* **36** 623

[7] P P Kane 1992 *Phys. Rep* **218** 67

[8] V Etalaniemi, K Hamalainen, S Manninen, P Suortti, S P Collins, M J Cooper and P P Kane 1988 *IX Sagamore Conference* Portugal (unpublished)

[9] P Eisenberger, P M Platzman and H Winick 1976 *Phys. Rev.* **B13** 2377

[10] K Hamalainen, S Manninen, S P Collins and M J Cooper 1990 *J Phys. (Lond.) · Cond. Matter.* **2** 5619

[11] A Kodre and S M Shafroth 1979 *Phys. Rev.* **A19** 675

[12] S Manninen, N G Alexandropoulus and M J Cooper 1985 *Phil. Mag* **B52** 899

[13] D H Schaupp, F Smend, R Wenskus, M Schumacher, A M Millhouse and H Schenk-Strauss 1984 *Z Physik* **A319** 1

[14] S Manninen 1986 *Phys. Lett* **57** 1500

[15] A Kodre, M Hribar and D Glavic 1986 *Z. Physik* **D2** 177